



SCUOLA INTERNAZIONALE SUPERIORE DI STUDI AVANZATI

SISSA Digital Library

Possible existence of wormholes in the central regions of halos

Original

Availability:

This version is available at: 20.500.11767/14253 since:

Publisher:

Published

DOI:10.1016/j.aop.2014.08.003

Terms of use:

Testo definito dall'ateneo relativo alle clausole di concessione d'uso

Publisher copyright

note finali coverpage

(Article begins on next page)

17 April 2024

Possible existence of wormholes in the central regions of halos

Farook Rahaman

Department of Mathematics, Jadavpur University, Kolkata 700032, West Bengal, India
rahaman@iucaa.ernet.in

P. Salucci

SISSA, International School for Advanced Studies, Via Bonomea 265, 34136, Trieste, Italy and INFN, Sezione di Trieste, Via Valerio 2, 34127, Trieste, Italy
salucci@sissa.it

P.K.F. Kuhfittig

Department of Mathematics, Milwaukee School of Engineering, Milwaukee, Wisconsin 53202-3109, USA
kuhfitti@msoe.edu

Saibal Ray

Department of Physics, Government College of Engineering & Ceramic Technology, Kolkata 700010, West Bengal, India
saibal@iucaa.ernet.in

Mosieur Rahaman

Department of Mathematics, Meghnad Saha Institute of Technology, Kolkata 700150, India
mosieurju@gmail.com

Abstract

An earlier study [1, 2] has demonstrated the possible existence of wormholes in the outer regions of the galactic halo, based on the Navarro-Frenk-White (NFW) density profile. This paper uses the Universal Rotation Curve (URC) dark matter model to obtain analogous results for the central parts of the halo. This result is an important compliment to the earlier result, thereby confirming the possible existence of wormholes in most of the spiral galaxies.

Keywords: General Relativity; universal rotation curves; wormholes

1. Introduction

Wormholes are hypothetical handles or tunnels in spacetime linking widely separated regions of our Universe or entirely different universes. Morris and Thorne [3] proposed the following line element for the wormhole spacetime:

$$ds^2 = -e^{2f(r)} dt^2 + \left(1 - \frac{b(r)}{r}\right)^{-1} dr^2 + r^2(d\theta^2 + \sin^2\theta d\phi^2), \quad (1)$$

using units in which $c = G = 1$. Here $f = f(r)$ is called the *redshift function*, which must be everywhere finite to prevent an event horizon. The function $b = b(r)$ is called the *shape function*, which has the property that $b(r_{th}) = r_{th}$, where $r = r_{th}$ is the *throat* of the wormhole. A key requirement is the *flare-out condition* at the throat: $b'(r_{th}) < 1$, while $b(r) < r$ near the throat. The flare-out condition can only be satisfied by violating the null energy condition (NEC), which states that $T_{\mu\nu}k^\mu k^\nu \geq 0$ for all null vectors and where $T_{\mu\nu}$ is the energy-momentum tensor. So given the null vector $(1, 1, 0, 0)$, the NEC is violated if $\rho + p_r < 0$, where ρ is the energy density and p_r the radial pressure.

The possible existence of wormholes in the outer region of the halo has already been discussed in Refs. [1, 2] using the Navarro-Frenk-White (NFW) density profile [4]:

$$\rho(r) = \frac{\rho_s}{\frac{r}{r_s} \left(1 + \frac{r}{r_s}\right)^2},$$

where r_s is the characteristic scale radius and ρ_s is the corresponding density. This model yields a shape function whose basic properties, such as the throat size, remain the same in the region considered [2]. It is well known that the NFW model predicts velocities in the central parts that are too low [5], but these discrepancies do not exist in the outer regions of the halo where the wormholes discussed in Refs. [1, 2] are located [6, 7].

In this study we are going to be primarily concerned with the region closer to the center where the Universal Rotation Curve (URC) dark matter profile is valid [8]:

$$\rho(r) = \frac{\rho_0 r_0^3}{(r + r_0)(r^2 + r_0^2)}; \quad (2)$$

here r_0 is the core radius and ρ_0 the effective core density. While the URC model is valid throughout the halo region, we assume that the outer region has already been dealt with in Refs. [1, 2] using the NFW model, thereby leaving only the central region, which is the subject of this paper.

In this connection we would like to add here that the URC represents any single rotation curve in spirals of any mass and Hubble type, and it is an obvious step forward with respect to assuming a constant value. At some time, a Cored Burkert profile is a step forward with respect to NFW profile that, it is now common fact that the latter fails to reproduce the Dark Matter distribution. Both the URC and the Cored profile are born empirically and find some explanation later on [9].

Therefore, our plan of the present work is as follows: In Sec. 2 we provide the basic equations and their solutions under the URC dark matter profile whereas Sec. 3 is devoted for some specific comments regarding the results obtained in the study.

2. The basic equations and their solutions

Even though we now have the density profile, other properties of dark matter remain unknown. So we are going to assume that dark matter is characterized by the general anisotropic energy-momentum tensor [10]

$$T_{\nu}^{\mu} = (\rho + p_t)u^{\mu}u_{\nu} - p_t g_{\nu}^{\mu} + (p_r - p_t)\eta^{\mu}\eta_{\nu}, \quad (3)$$

with $u^{\mu}u_{\mu} = -\eta^{\mu}\eta_{\mu} = -1$, p_t and p_r being the transverse and radial pressures, respectively. The line element for the galactic halo region is given in Eq. (1).

The flat rotation curve for the circular stable geodesic motion in the equatorial plane yields the tangential velocity [11, 12]

$$(v^{\phi})^2 = r f'(r). \quad (4)$$

The radius r in kpc and velocity v^{ϕ} in km/s of the Rotation Curve of objects with total virial mass 3×10^{12} solar masses is given below (Table - 1) [9]. We find the best fitting curve which is given in Fig. 1.

By applying intuition, we propose that the observed rotation curve profile in the dark matter region is of the form

$$v^{\phi} = \alpha r \exp(-k_1 r) + \beta[1 - \exp(-k_2 r)]. \quad (5)$$

For a typical galaxy the tangential velocity v^ϕ is shown in Fig. 1. Moreover, for sufficiently large r , $v^\phi \sim 250 \text{ km/s} \approx 0.00083$ [13, 14]. One can note that our proposed curve and observed curve profile for tangential velocity are almost similar to each other for the specific values of the parameters i.e. the proposed and observed rotational velocities are both fittable with our empirical formula. Therefore, our assumption is more or less justified.

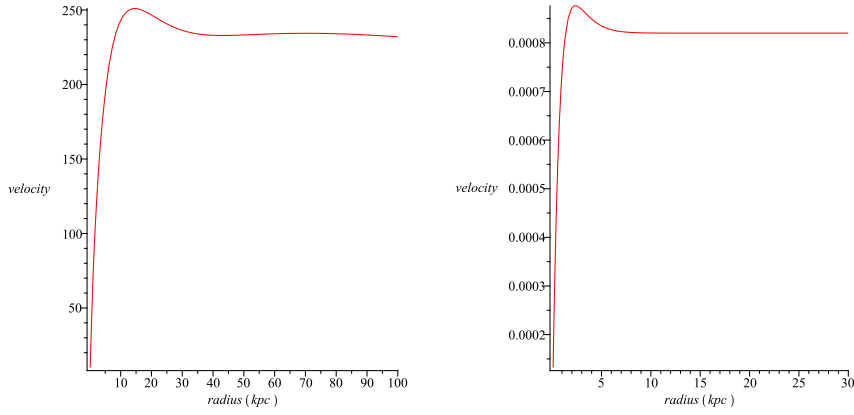


Figure 1: (Left) The rotational velocity from observations. (Right) The proposed rotational velocity with the values of the parameters as $k_1 = k_2 = 1$, $\alpha = 0.0006$, $\beta = 0.00082$.

Table 1: The radius r in kpc and velocity v^ϕ in km/s of the Rotation Curve of objects with total virial mass 3×10^{12} solar masses.

R (kpc)	V (km/s)	R (kpc)	V (km/s)
0.1	10.052834744388612	26.1	239.5389556726835
1.1	74.46665498068327	27.1	238.58964093528954
2.1	118.22330294498593	28.1	237.72382676461396
3.1	151.1128881336094	29.1	236.94252666484462
4.1	176.44533836937705	30.1	236.24478171375338
5.1	196.0988184186591	31.1	235.62813232944393
6.1	211.33095938495612	32.1	235.08901162538888
7.1	223.05674521744098	33.1	234.62307027076736
8.1	231.97462265975628	34.1	234.62307027076736
9.1	238.63397717705232	35.1	234.22544187966773
10.1	243.47545965729188	36.1	233.89095712722872
11.1	246.8570877004846	37.1	233.39021089298888
12.1	249.07218340068806	38.1	233.2134483391877
13.1	250.36228653986132	39.1	233.07900487106537
14.1	250.92679861285606	40.1	232.98209135254623
15.1	250.93040201908613	41.1	232.91818791468324
16.1	250.5089080065525	42.1	232.88306686283582
17.1	249.77395990965775	43.1	232.87280446959267
18.1	248.81687987924815	44.1	232.88378410156642
19.1	247.71185949364315	45.1	232.91269272147773
20.1	246.51863692196736	46.1	232.95651245084068
21.1	245.2847642472647	47.1	233.0125085700085
22.1	244.04754149102484	48.1	233.07821506796643
23.1	242.8356747965165	49.1	233.15141862990475
24.1	241.67070261276308	50.1	233.23014176204364
25.1	240.56822394226268		

The Einstein field equations for the above metric are

$$\frac{b'(r)}{r^2} = 8\pi\rho(r), \quad (6)$$

$$2\left(1 - \frac{b}{r}\right)\frac{f'}{r} - \frac{b}{r^3} = 8\pi p_r(r), \quad (7)$$

$$\left(1 - \frac{b}{r}\right)\left[f'' + \frac{f'}{r} + f'^2 - \left\{\frac{b'r - b}{2r(r-b)}\right\}\left(f' + \frac{1}{r}\right)\right] = 8\pi p_t(r). \quad (8)$$

From Eqs. (4) and (5) and using some typical values, we obtain the redshift function

$$f(r) = -\frac{\alpha^2 r}{2k_1 e^{(2k_1 r)}} - \frac{\alpha^2}{4k_1^2 e^{(2k_1 r)}} - \frac{2\alpha\beta}{k_1 e^{(k_1 r)}} + \frac{2\alpha\beta e^{(-k_1 r - k_2 r)}}{k_1 + k_2} + \beta^2 \ln(r) + 2\beta^2 E_i(1, k_2 r) - \beta^2 E_i(1, 2k_2 r) + D. \quad (9)$$

Here $E_i(*, *)$ is the exponential integral and D is an integration constant. The graph of $f(r)$ in Fig. 2 shows the behavior in the central part of the halo, which is the region that we are primarily concerned with. (For large r , $f(r)$ is such that $e^{2f(r)} = B_0 r^l$ where $l = 2(v^\phi)^2$ [13, 14]).

The determination of the shape function $b = b(r)$ requires a little more care. First of all, we assume that $b(r)$, $f(r)$, and the halo have a common origin in order to use Eqs. (4) and (6) in the calculations. To see if the shape function meets the basic requirements, we start with Eq. (6),

$$b'(r) = 8\pi r^2 \rho(r),$$

and integrate from 0 to r to obtain

$$b(r) = 4\pi r_0^3 \rho_0 \ln(r + r_0) + 2\pi r_0^3 \rho_0 \ln(r^2 + r_0^2) - 4\pi \rho_0 r_0^3 \tan^{-1}\left(\frac{r}{r_0}\right) + C, \quad (10)$$

where C is an integration constant. To get an overview of the shape function, we assign some arbitrary values to the parameters and obtain the plots in Fig.2 shows that the throat is located at some $r = r_{th}$, where $b(r) - r$ intersects the r -axis. Also, for $r > r_{th}$, $b(r) - r < 0$, which implies that $b(r)/r < 1$. Furthermore, $b(r) - r$ is decreasing for $r \geq r_{th}$, implying that $b'(r_{th}) < 1$. Hence the flare-out condition is satisfied. So based on the URC model, the qualitative features meet all the requirements for the existence of a wormhole.

At this point it would be desirable to examine the effect of using more specific parameters. For example, if the throat of the wormhole coincides with the core radius $r = r_0$, then we get for the shape function

$$\begin{aligned} b(r) &= \int_{r_0}^r 8\pi r^2 \rho dr + r_0 \\ &= 4\pi r_0^3 \rho_0 \ln(r + r_0) + 2\pi r_0^3 \rho_0 \ln(r^2 + r_0^2) - 4\pi \rho_0 r_0^3 \tan^{-1}\left(\frac{r}{r_0}\right) + C, \end{aligned} \quad (11)$$

where

$$C = r_0 - 4\pi r_0^3 \rho_0 \ln 2r_0 - 2\pi r_0^3 \rho_0 \ln 2r_0^2 + \pi^2 \rho_0 r_0^3.$$

As before, $b(r_0) = r_0$.

Having determined the throat radius allows a closer look at the flare-out condition, which again depends on $b'(r)$. By Eqs. (6) and (2),

$$b'(r) = 8\pi r^2 \frac{\rho_0 r_0^3}{(r + r_0)(r^2 + r_0^2)}. \quad (12)$$

In the specific case of the Milky Way galaxy, $r_0 = 9.11$ kpc [7] and $\rho_0 = 5 \times 10^{-24} (r_0/8.6 \text{ kpc})^{-1} \text{ g cm}^{-3}$ [8]. Substituting in Eq. (12), we get

$$b'(r_0) \approx 1.74 \times 10^{-6}.$$

The flare-out condition is easily satisfied. Notice that this result does not change if we adopt the Milky Way values for ρ_0 and r_0 found by the accurate analysis of [16]

To complete our discussion, we will use Eqs. (7) and (8) to obtain the radial and lateral pressures:

$$p_r(r) = \frac{1}{8\pi r^3} [2(r - A)B^2 - A], \quad (13)$$

$$\begin{aligned} p_t(r) &= \frac{1}{8\pi} \left(1 - \frac{A}{r}\right) \times \\ &\left[\frac{2B\{\alpha e^{(-k_1 r)} - \alpha r k_1 e^{(-k_1 r)} + \beta k_2 e^{(-k_2 r)}\}}{r} + \frac{B^4}{r^2} - \frac{\left(\frac{8\pi \rho_0 r^6}{(r+r_0)(r^2+r_0^2)} - A\right) \left(B^2 + \frac{1}{r}\right)}{2r^2(r-A)} \right]. \end{aligned} \quad (14)$$

where

$$A = 4\pi r_0^3 \rho_0 \ln(r + r_0) + 2\pi r_0^3 \rho_0 \ln(r^2 + r_0^2) - 4\pi r_0^3 \rho_0 \tan^{-1}\left(\frac{r}{r_0}\right) + C,$$

$$B = v^\phi = \alpha r e^{(-k_1 r)} + \beta [1 - e^{(-k_2 r)}].$$

According to Fig. 3, $\rho + p_r < 0$, so that the null energy condition is indeed violated.

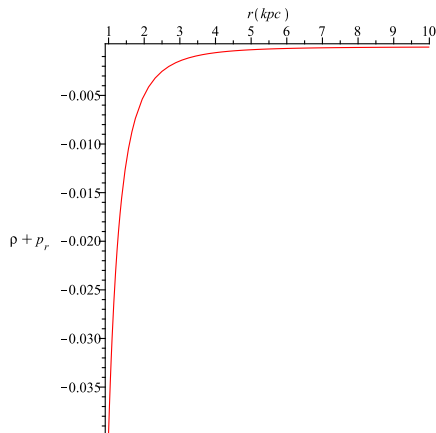


Figure 2: Plot showing that $\rho + p_r < 0$ for values of the parameters $r_0 = 1, \rho_0 = 0.0001$

3. Concluding remarks

The possible existence of wormholes in the outer regions of the halo was discussed in Ref. [1], based on the NFW density profile. Possible detection by means of gravitational lensing, discussed in Ref. [2], has shown that the basic features, such as the throat size, are independent of the position within the halo. Because of certain discrepancies discovered near the center, this paper uses the observationally motivated URC dark matter density profile instead in order to accommodate the region closer to the center of the halo. This center is also the center of the wormhole.

It is subsequently shown that the solution obtained satisfies all the criteria for the existence of a wormhole, particularly the violation of the null energy condition. In the special case of the Milky Way galaxy, if the throat

radius $r = r_0$ coincides with the radius of the core, then $b'(r_0) \approx 1.74 \times 10^{-6}$, thereby meeting the flare-out condition. A similar result can be expected for most spiral galaxies. Thus our result is very important because it confirms the possible existence of wormholes in most of the spiral galaxies. Scientists remain silent on whether it is possible to manufacture or create of the exotic matter violating null energy condition in laboratory. As a result the construction of a wormhole geometry in our real world is extremely difficult. However in the galactic halo region, dark matter may supply the fuel for constructing and sustaining a wormhole. Hence, wormholes could be found in nature and our study may encourage scientists to seek observational evidence for wormholes in the galactic halo region.

Acknowledgments

FR and SR are thankful to the Inter-University Centre for Astronomy and Astrophysics (IUCAA), India for providing Associateship Programme where a part of the work has been done. FR is also grateful to Jadavpur University, India for financial support.

References

- [1] F. Rahaman, P.K.F. Kuhfittig, S. Ray, N. Islam, *Eur. Phys. J. C* **74**, 2750 (2014)
- [2] P.K.F. Kuhfittig, *Eur. Phys. J. C* **74**, 2818 (2014)
- [3] M.S. Morris, K.S. Thorne, *Am. J. Phys.* **56**, 395 (1988)
- [4] J.F. Navarro, C.S. Frenk, S.D.M. White, *Astrophys. J.* **462**, 563 (1996)
- [5] G. Gentile, P. Salucci, U. Klein, D. Vergani, P. Kalberla, *MNRAS* **351**, 903 (2004)
- [6] C. Tonini, A. Lapi, P. Salucci, *Astrophys. J.* **649**, 591 (2006).
- [7] A.V. Maccio, et al., *ApJ Lett.* **744**, L9 (2012)
- [8] G. Castignani, N. Frusciante, D. Vernieri, P. Salucci, *Nat. Sci.* **4**, 265 (2012)

- [9] P. Salucci, A. Lapi, C. Tonini, G. Gentile, I. Yegorova, U. Klein, MNRAS **378**, 41 (2007); Persic, M. Salucci, P. Stel, F. 1996, MNRAS, 281, 27
- [10] N. Bozorgnia et al, JCAP *1312*, 050 (2013)
- [11] S. Chandrasekhar, Mathematical Theory of Black Holes (Oxford Classic Texts, 1983)
- [12] L.D. Landau and E.M. Lifshitz, The Classical Theory of Fields (Oxford, Pergamon Press, 1975)
- [13] F. Rahaman, M. Kalam, A. De Benedictis, A.A. Usmani, S. Ray, MNRAS **27** 389 (2008)
- [14] K.K. Nandi, A.I. Filippov, F. Rahaman, S. Ray, A.A. Usmani, M. Kalam, A. De Benedictis, MNRAS **399**, 2079 (2009)
- [15] J. Ponce de León, Gen. Relativ. Gravit. **25**, 1123 (1993)
- [16] Nesti, F.; Salucci, P, MNRAS **7**, 16 (2013)

